Korea-Australia Rheology Journal, Vol.24, No.3, pp.249-253 (2012) www.springer.com/13367
DOI: 10.1007/s13367-012-0030-1

Short Communications

Conformational transition of polyelectrolyte chains extending over the de Gennes regime in slitlike nanochannels

Myung-Suk Chun*
Complex Fluids Laboratory, National Agenda Res. Div., Korea Institute of Science and Technology (KIST), Seongbuk-gu, Seoul 136-791, Republic of Korea

(Received September 11, 2012; final revision received September 16, 2012; accepted September 18, 2012)

The confinement-induced conformational transitions of the polyelectrolyte chain are characterized with the coarse-grained Brownian dynamics simulations and the blob theory. Submicron-sized biopolymer xanthan is chosen as a model polyelectrolyte taking into account both flexible and semiflexible chains for comparison. Confined flexible and semiflexible chains exhibit a nonmonotonic variation in size in weak confinements, where the relative radius of gyration shows a dip and then increases when decreasing the channel width. The rigid chain, realized at low screening, exhibits a sigmoidal transition without minima in size. Major attention should be on the dependence of scaling law exponents on the screening effect of the solution in the moderate confinement of the de Gennes regime. Our findings are expected to provide useful information and new insight into the confined polyelectrolytes when relevant micro/nanochannels are designed and fabricated.

***Keywords*:** polyelectrolyte, conformation, nanochannel, de Gennes regime, blob theory

Introduction

Polyelectrolytes, which take charged polymer chains (macroions) and mobile counterions, are distinguished from neutral polymers. A thorough understanding of soft matters has become of great attention in biophysics and single molecule studies, because virtually all proteins and other biopolymers, such as DNA and polysaccharide, are polyelectrolytes. Polyelectrolytes in confined spaces exhibit altered structure and dynamics compared to their behavior in bulk solutions due to their interaction with bounding surfaces [Peter and Kremer, 2010; Wyatt and Liberatore, 2010]. Note that confinement-induced changes have practical relevance to the development of high-throughput micro total analysis system (μTAS), *inter alia*, DNA sequencing, genome analysis, and cell counting/sorting [Mannion *et al.*, 2006; Strychalski *et al.*, 2012]. Although advancements in nanofabrication techniques provide an attractive route to develop various complex geometries, slit channels have received the majority of attention due to acting as a prototype example of uniaxial confinement [Thamdrup *et al.*, 2008; Persson *et al*., 2009].

Regarding the issue of slitlike confinement, three primary regimes can be identified by being dependent on a competition between three length scales with the three dimensional (3D) radius of gyration R_g^{bulk} in bulk, the persistence length l_p, and the channel width $2Z_o$. In a weakly confined regime where $2Z_o \geq nR_g^{bulk}$ ($n > 1$), the polyelectrolyte coil is slightly perturbed by the presence of the wall. A condition of $l_p << 2Z_o < R_g^{bulk}$ provides the moderately confined regime (cf., known as the de Gennes regime). In the usual situation of a good solvent, confinement of polyelectrolyte chain in one or two directions leads to chain expansion in the unconfined dimensions. As shown in Fig. 1, the excluded volume interaction is represented by a string of blobs, where a blob is a subchain of connected segments with correlated behavior [Daoud and de Gennes, 1977; de Gennes 1979; Teraoka 1996; Hsieh and Doyle 2008]. A blob with diameter $2Z_o$ has about $(2Z_o/l_p)^{5/3}$ segments and thus there are N_{bl} ($\sim (R_C/l_p)/(2Z_o/l_p)^{5/3}$) blobs in the chain with contour length R_C. Subsequently, the overall average chain expansion is determined by assuming a self-avoiding random walk with step length $2Z_o$ in unconfined directions. In a strongly confined regime where $l_p \sim 2Z_o << R_g^{bulk}$ (cf., known as Odijk regime), the blob description breaks down, because the orientational and translational freedom become restricted at the length scale of a statistical segment [Odijk, 2008]. In this, polyelectrolyte conformation in the direction perpendicular to the slit wall can be described by the deflection chain model.

The current study aims at examining of polyelectrolyte conformation in slitlike confinement. From the coarse-grained mesoscale simulations, we show that the different behavior between flexible and semiflexible chains and the screening effect on the blob model in moderate confinement. Polysaccharide xanthan is applied as a model poly-

This paper is a part of the invited lecture presented at the 12th International Symposium on Applied Rheology (ISAR), held May 17, 2012, Seoul.
*Corresponding author: mschun@kist.re.kr

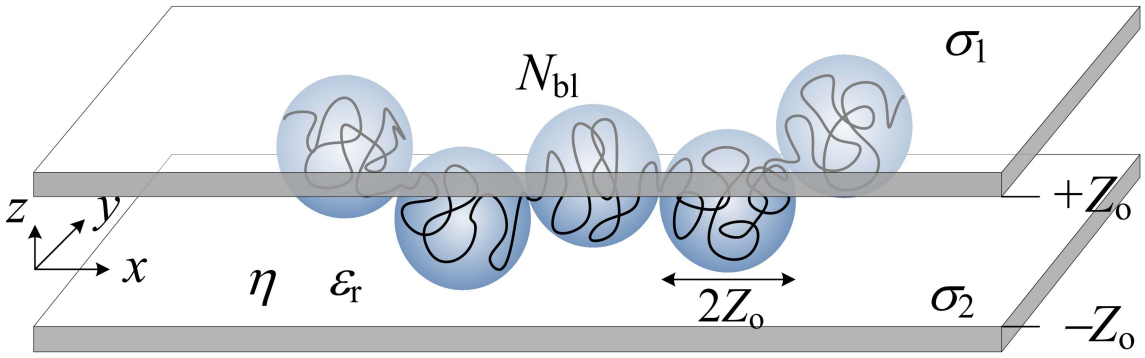

Fig. 1. (Color online) Polyelectrolyte chain in moderately confined channel of a de Gennes regime, representing the blobs of chain segments.

electrolyte, which has up to two ionizable carboxyl groups per repeat unit and the side chains give a semirigid character. The extension of native xanthan at low ionic strength and a corresponding increase in the solution viscosity are likely to involve a transition of the backbone conformation from a semiflexible double strand to a disordered flexible form with lower strandedness [Rochefort and Middleman, 1987; Camesano and Wilkinson, 2001]. This denatured xanthan can undergo a disorder→order (i.e., coil→helix) transition when sufficient salt is present. Previous studies of the present work are those of Jeon and Chun (2007) and Chun (2008), who studied the structural transition of a chain from unbounded to confined states with emphasis on the influence of chain intrinsic rigidity.

Coarse-Grained Mesoscale Simulations of Confined Polyelectrolytes in Solvent

The Brownian dynamics (BD) simulations are performed throughout, and we follow the coarse-grained bead-spring model of anionic polyelectrolyte xanthan as presented in the previous study [Jeon and Chun, 2007]. The coarse-graining neglects all detailed atomistic interactions that are replaced by effective interactions. The polyelectrolyte chain is considered to be divided into a finite number of beads, each of which fluctuates in length due to thermal excitations. Information on the dimension of the native xanthan, used in the previous studies, was presented as the average molecular weight of 1.13×10^6 g/mol with $l_p \cong 120$ nm and $R_C \cong 580$ nm at medium ionic strength $I = 100$ mM. Considering the ratio of R_C/l_p, xanthan can be modeled as a mesoscopic discrete wormlike chain with 25 beads ($N_b = 25$) connected by N_b-1 springs, and 10 beads approximately represent a Kuhn length ($= 2l_p$).

The dynamics of the xanthan chain is described by the following stochastic equation [Ermak and McCammon, 1978] that accounts for the bead-bead hydrodynamic interaction (HI)

$$\mathbf{r}_i^{n+1}-\mathbf{r}_i^n=\Delta t\sum_j \mathbf{D}_{ij}^n\cdot(-\nabla E_j^T(t_n)/k_BT)+\Delta t\sum_j\nabla_j\cdot\mathbf{D}_{ij}^n+\mathbf{R}_i^n \quad (1)$$

Here, $\mathbf{r}_i^n$ is the position of the i-th bead, $-\nabla E_j^T(t_n)$ is the total potential on the j-th bead at time t_n, $\mathbf{R}_i^n$ is the random displacement due to the solvent, Δt is the time step, and k_BT denotes the Boltzmann thermal energy. The velocity field created from the segmental motion of the xanthan molecule is exactly considered by implementing the bead-bead HI. The Rotne-Prager diffusion tensor $\mathbf{D}_{ij}^n$ is employed, in common with several recent workers. It is positive-definite for all chain configurations, expressed by $\mathbf{D}_{ij}=k_BT(\mathbf{I}\delta_{ij}/6\pi\eta a+\boldsymbol{\Omega}_{ij})$ with formulating 3×3 block components of the $3N_b \times 3N_b$ matrix. Here, η is the solvent viscosity, a is the bead hydrodynamic radius, $\mathbf{I}$ is the unit tensor, and Ω_{ij} is the HI tensor. HI relates to a velocity perturbation of a bead carried by the surrounding fluid at point $\boldsymbol{r}_i$ to a point force at $\boldsymbol{r}_j$. Brownian forces coupled to velocity perturbations through the fluctuation-dissipation theorem can effectively be approximated by the White noise process, where the distribution of $\mathbf{R}_i^n$ is Gaussian with a zero mean and a covariance.

In the total potential E^T, one needs to apply to the spring, bending, Lennard-Jones (LJ) potentials, and electrostatic interactions. We describe briefly here, since details are provided in our previous studies. The xanthan molecule is empirically represented by a bead-spring chain with the finitely extensible nonlinear elastic (FENE) model,

$$E_{i,i+1}^{\mathrm{FENE}}=-(k_s l_{\max}^2/2)\ln[1-(r_{i,i+1}-l_o)^2/l_{\max}^2] \quad (2)$$

where l_o is the equilibrium bond length and l_{max} is the maximum bond length allowed. E^{FENE} is reduced to a harmonic potential with force constant k_s, in the limit of large l_{max}. Intrinsically semiflexible and flexible chains are distinguished by each model with and without the bending potential, respectively. The finite rigidity of the chain is modeled by the harmonic bending potential, $E_{i,i+1}^{Bend}=k_A\theta_{i,i+1}/2$, where k_A is the bending force constant and $\theta_{i,i+1}=arc\cos(\hat{b}_i\cdot\hat{b}_{i+1})$ is the angle with the i-th bond vector of unit size $\hat{b}_i$. The LJ potential between pairs of beads is taken by introducing the energy parameter ($= k_BT$) and the length scale ($= l_o$).

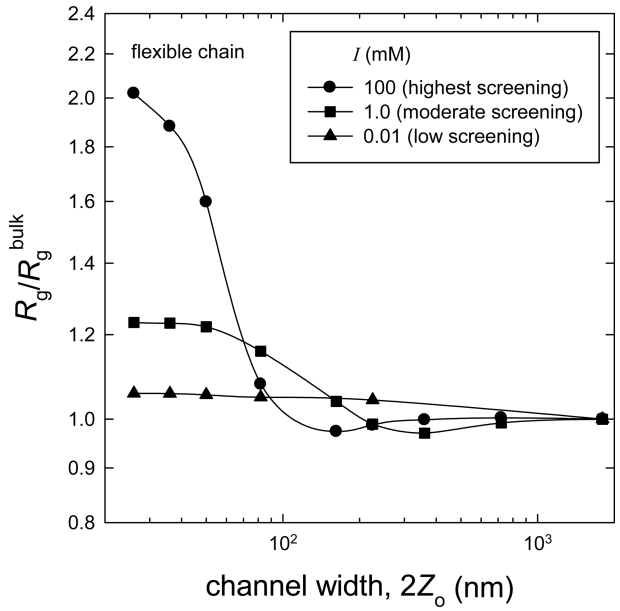

Fig. 2. Change of the relative radius of gyration R_g for confined flexible chain as a function of the slit width $2Z_o$ for different screening effects.

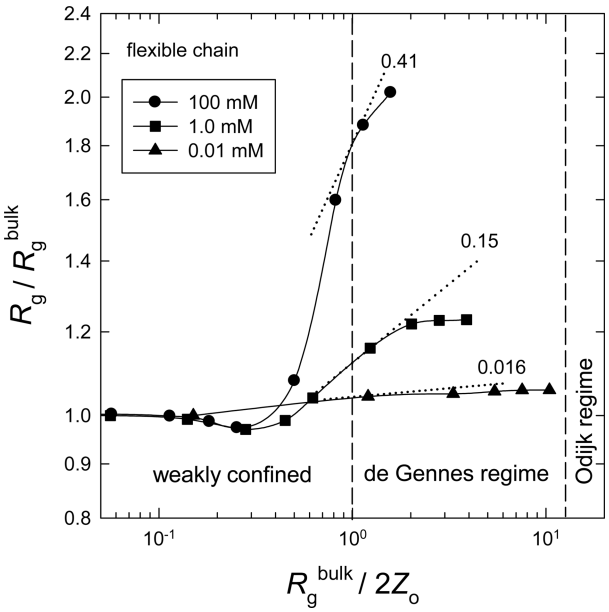

Fig. 3. Conformational transitions of confined flexible chain as a function of the inverse of relative slit width for different screening effects.

Involving the excluded volume effect, the long-range electrostatic interaction between beads with charge q_b is addressed via the screening Coulombic interaction, known as the Debye-Hückel (DH) potential $E_{ij}^{ES} = (q_b^2/4\pi\varepsilon_r\varepsilon_o)(e^{-\kappa r_{ij}}/r_{ij})$, where $r_{ij} = |\mathbf{r}_j - \mathbf{r}_i|$. The medium dielectric constant $\varepsilon_r\varepsilon_o$ is defined in terms of the relative permittivity ε_r (= 78.5 for water at 25°C) and vacuum permittivity ε_o, and κ denotes the inverse Debye screening thickness. As the bead-wall interaction for a confined chain, the steric repulsion is first specified as $E_i^{WR} = k_W/(|z_i| - Z_o)^2$ with $k_W = 2.5 l_o^2 k_B T$ and the half-width of the slit Z_o. Employing the DH interaction of a point charge with two infinite charged plates provides the electrostatic interaction E_i^{WES} of bead i with constant surface charge densities σ_1 at $z = Z_o$ and σ_2 at $z = -Z_o$

$$E^{WES} = \frac{q_b}{\varepsilon_r\varepsilon_o \kappa \sinh(2\kappa Z_o)}[\sigma_2 \cosh(\kappa(z_i - Z_o)) + \sigma_1 \cosh(\kappa(z_i + Z_o))] . \quad (3)$$

Here, z_i is the z coordinate of bead i perpendicular to the walls from the center of the slit. We consider the negatively charged polydimethylsiloxane channel, then the wall charge density σ_w (= $\sigma_1 = \sigma_2$) is chosen as -5.2×10^{-4} C/m^2, from the relationship of $\sigma_w = \varepsilon_r\varepsilon_o\kappa\zeta$ [Israelachvili, 1991] and the data of zeta potential ζ with assumption of the ionic strength independency of σ_w. Input parameters of the flexible and semiflexible models of xanthan were summarized as a Table in the previous works [Jeon and Chun, 2007; Chun, 2008], where simulation parameters and conditions were also described in detail.

Results and Conclusions

We estimate the radius of gyration $R_g = (N_b^{-1}\sum_{n=1}^{N_b}|\mathbf{r}_n - \mathbf{r}_{cm}|^2)^{1/2}$ ($\mathbf{r}_{cm} = N_b^{-1}\sum_{n=1}^{N_b}\mathbf{r}_n$) of flexible and semiflexible xanthan confined in slits. In the log-log plot of Fig. 2, the minima appear at a larger slit width with decreasing screening effect, and the minima are suppressed at low screening and the chain exhibits a sigmoidal transition instead. Screening effect is controlled by applying different ionic concentrations in the solution, where the screening thickness $\kappa^{-1} = [\varepsilon_r\varepsilon_o k_B T/(N_A e^2 \sum_i \Lambda_i^2 I)]^{1/2}$ is determined by Avogadro's number N_A, the elementary charge e, I (mM), and the valence of i ions Λ_i. I (mM) of 100, 1.0, and 0.01 result in κ^{-1} of 0.97, 9.7, and 97 nm around the beads. Previous studies revealed that the reduction in chain size at an intermediate confinement is accompanied by a severe loss of the long-range bond vector correlation measured by l_p at a long length scale.

In order to understand in-depth the conformational transition, the slit width is normalized by R_g^{bulk} and three regimes are divided, as shown in Fig. 3. The vertical lines are used as the lower and upper bounds for the de Gennes regime. In weak confinement, the 3D radius of gyration of a chain shows a dip and then increases when decreasing the channel width, agreeing with the theoretical prediction [Cordeiro *et al.*, 1997; Tang *et al.*, 2010]. Note that this nonmonotonic behavior of xanthan structure is caused by a competition between swelling in the x–y plane and compression in the z-direction. The moderate confinement (i.e., de Gennes regime) exhibits a linear behavior, which cor-

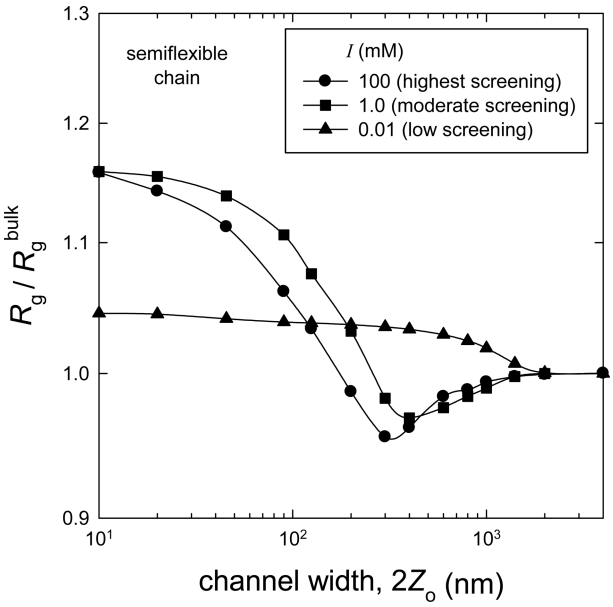

Fig. 4. Change of the relative radius of gyration R_g for confined semiflexible chain as a function of the slit width $2Z_o$ for different screening effects.

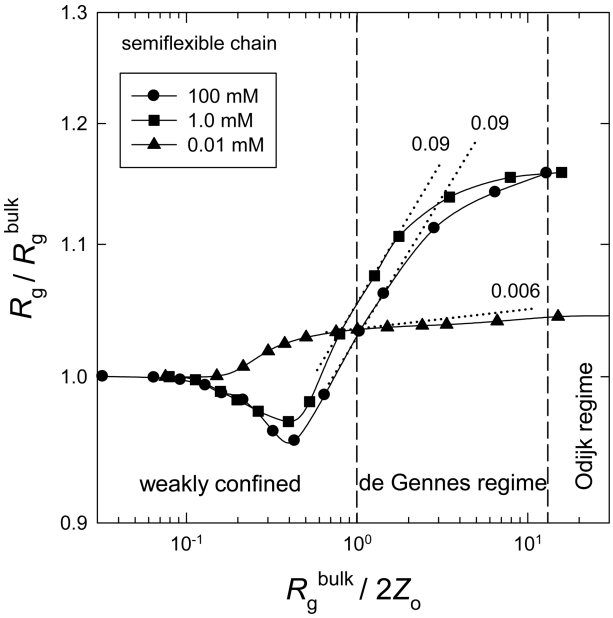

Fig. 5. Conformational transitions of confined semiflexible chain as a function of the inverse of relative slit width for different screening effects.

responds to the scaling law according to the blob theory. The dotted lines are the best fits for power scaling $R_g/R_g^{bulk} \simeq (R_g^{bulk}/2Z_o)^{\alpha}$ with an exponent α to the simulation data on the vertical line. It provides the slopes in terms of α as 0.41, 0.15, and 0.016 for each screening case, where the average uncertainties of α are about ±10%.

Figs. 4 and 5 display simulation results of the conformational transitions of semiflexible xanthan. The sigmoidal transitions at low screening and the nonmonotonic variations at intermediate and high screening are equally preserved as in the flexible xanthan. Compared to the flexible chain, the magnitude of R_g/R_g^{bulk} decreases evidently at high screening. Sigmoidal transitions are related to the fact that the xanthan chain becomes rigid at low screening (I = 0.01 mM) due to the intrachain electrostatic repulsion. Power scaling exponents α estimated by the best fits to the simulation data are obtained as 0.09, 0.09, and 0.006 for each screening case.

It is possible to admit apparent configurations of the in-plane 2D polymer size (i.e., projection on the confining slit walls). In moderate confinement with in-plane 2D case, simulations of equilibrium in-plane radius of gyration for chain consistently show the expected power law scaling [Cifra *et al.*, 2008]: $R_{g,2D}$ (or root-mean-square end-to-end distance) scales as $2Z_oN_{bl}^{3/4}$. From the Flory theory, equilibrium chain conformations in a good solvent scale as $l_p(R_C/l_p)^{\nu}$, where ν= 3/5 and 1/4 for $R_{g,2D}^{bulk}$ ($R_{g,2D}$ in bulk) and $R_{g,2D}^{plane}$ ($R_{g,2D}$ confined to a plane), respectively. As a result, each scaling for $R_{g,2D}$ in the de Gennes and the Odijk regimes becomes respectively as

$$R_{g,2D}/R_{g,2D}^{bulk} \simeq (R_{g,2D}^{bulk}/2Z_o)^{1/4}, \quad (4)$$

$$R_{g,2D}/R_{g,2D}^{plane} \simeq (l_p/2Z_o)^{1/4}. \quad (5)$$

In the present study, conformational transitions of flexible and semiflexible polyelectrolytes in slitlike confinement have been explored by using the scaling theory and BD simulations. The screening effect dependence on the scaling exponents was newly found from the normalized plots between the 3D R_g and the inverse slit width. Our results are not only of fundamental importance to understanding of the interactions between confinement and conformational dynamics, but also useful in the design platform aiming to exploit confinement to manipulate polyelectrolyte soft matters.

This work was supported by Basic Science Research Program through the National Research Foundation (NRF) of Korea funded by the Ministry of Education, Science, and Technology (No. 2012-0007164) and the Future-Oriented Research Fund (No. 2E22861) from the KIST.

References

Camesano, T.A. and K.J. Wilkinson, 2001, *Biomacromolecules* **2**, 1184.

Chun, M.-S., 2008, *J. Korean Phys. Soc.* **53**, 3404.

Cifra, P., Z. Benkova, and T. Bleha, 2008, *Faraday Discuss*. **139**, 377.

Cordeiro, C.E., M. Molisana, and D. Thirumalai, 1997, *J. Phys.*

II **7**, 433.
Daoud, M. and P.G. de Gennes, 1977, *J. Phys. Paris* **38**, 85.
de Gennes, P.G., 1979, *Scaling Concepts in Polymer Physics*, Cornell Univ. Press, Ithaca.
Ermak, D.L. and J.A. McCammon, 1978, *J. Chem. Phys*. **69**, 1352.
Hsieh, C.C. and P.S. Doyle, 2008, *Korea-Aust. Rheol. J*. **20**, 127.
Israelachvili, J.N., 1991, *Intermolecular and Surface Forces*, 2nd Ed., Academic Press, New York.
Jeon, J. and M.-S. Chun, 2007, *Korea-Aust. Rheol. J*. **19**, 51.
Mannion, J.T., C.H. Reccius, J.D. Cross, and H.G. Craighead, 2006, *Biophys. J*. **90**, 4538.
Odijk, T., 2008, *Phys. Rev. E* **77**, 060901.
Persson, F., P. Utko, W. Reisner, N.B. Larsen, and A. Kristensen, 2009, *Nano Lett*. **9**, 1382.
Peter, C. and K. Kremer, 2010, *Faraday Discuss*. **144**, 9.
Rochefort, W.E. and S. Middleman, 1987, *J. Rheol*. **31**, 337.
Strychalski, E.A., J. Geist, M. Gaitan, L.E. Locascio, and S.M. Stavis, 2012, *Macromolecules* **45**, 1602.
Tang, J., S.L. Levy, D.W. Trahan, J.J. Jones, H.G. Craighead, and P.S. Doyle, 2010, *Macromolecules* **43**, 7368.
Teraoka, I., 1996, *Prog. Polym. Sci*. **21**, 89.
Thamdrup, L.H., A. Klukowska, and A. Kristensen, 2008, *Nanotechnology* **19**, 125301.
Wyatt, N.B. and M.W. Liberatore, 2010, *Soft Matter* **6**, 3346.